DEVELOPMENT OF A 180° HYBRID BALUN TO FEED A TIGHTLY COUPLED DIPOLE X-BAND ARRAY

Senior Honors Thesis

Presented in Partial Fulfillment of the Requirements for Graduation with Distinction in the College of Engineering of The Ohio State University

By

Nathanael J. Smith

The Ohio State University

2010

Honors Thesis Committee:

Dr. John Volakis, Adviser

Dr. Chi-Chih Chen, Co-Adviser

Abstract

In contrast to conventional arrays, tightly coupled dipole arrays have been shown to provide enhanced broadband (4:1 performance) when placed near a conductive ground plane. However, such arrays cannot practically realize their full bandwidth with integrated feeding elements due to current design limitations. Such feeds also do not fully address the common mode problem which occurs at certain frequencies in the active array. In this effort, we propose and study several feed designs aimed at creating a wide band 180° hybrid balun. It is demonstrated that shielded structures that are not wavelength restrictive can be realized without exciting the troublesome common mode. The presented balun design provides a transition from 100Ω fed twin wire to 50Ω dual enclosed printed stripline that feeds the densely populated dipole array.

Acknowledgments

The author would like to thank Doctorial Candidate Mr. Justin Kasemodel for his time in training the author, and helpful discussions which were instrumental in my pursuit of this undergraduate research and the compilation of this thesis. Thanks also goes to Dr. John Volakis and Dr. Chi-Chih Chen for their mentoring through this research. Thanks to The Ohio State University for a scholarship grant to pursue this research as well as my friends and family that were supportive and helped with the proofreading of this thesis.

Vita

1986 ..... Born

2010 ..... B.S. Electrical & Computer Engineering
The Ohio State University
Columbus, OH

Fields of Study

Major Field: Electrical and Computer Engineering

Studies in:
Computers
Analog Circuits
Electromagnetism

Table of Contents

List of Figures

CHAPTER 1: INTRODUCTION

1.1. Motivation

As technology advances, it becomes increasingly desirable to create electrically smaller, cheaper, lower profile, and wider band antennas. In the world of integrated circuits, miniaturized and more powerful computer systems have made phenomenal advancements in the last decade. However, antenna design and performance has yet to achieve impressive size reductions in this period of time. There are both theoretical and fabrication challenges of modern technology that need to be overcome in order to allow for further miniaturization of antennas.

This paper is concerned with developing a wide band balun transformer to feed a low profile X-band (7GHz – 12.5GHz) tightly coupled dipole array (TCDA) preferably for dual polarization operation over a bandwidth of 4:1 or better. Current design methodologies allow feeding a TCDA over a bandwidth of approximately 1.6:1 while maintaining exceptional scan performance for X-band [1]. The advantage of the TCDA over other arrays, such as a Vivaldi antenna array, is how low profile the dipole array is in comparison. A Vivaldi array requires significant length in the z direction in order to obtain wide band performance. Tightly coupled dipole arrays obtain their wide band performance from mutual coupling due to neighboring elements canceling the ground plane reactance [4-5]. As a result, the difficulties in developing a balun feed for this application include small space requirements, especially in the z direction, wide bandwidth, and simplicity required for reproduction and cost.

1.2. Background

The word “balun” is an acronym literally meaning balanced-unbalanced and used as an intermediator for converting electrical signals between a balanced device to an unbalanced one and vice versa. In short, a single-ended signal is changed to a balanced signal with equal potentials with respect to ground but opposite polarity [2]. A balun can double as a means to convert one impedance value to another, allowing a more precise and accurate impedance match when connecting two RF devices together. If a balun is not used when required, not only will the antenna radiate, but the cable feeding the antenna will also become part of the antenna and radiate. This can cause interference with other equipment, as well as diminish the performance of the antenna. Due to the transitions of balanced to unbalanced systems, baluns are fundamental and necessary feeding elements for many different types of antennas.

The dipole antenna is a balanced system, however the coaxial cable which feeds the antenna is inherently unbalanced. Since the inner and outer conductors of the coaxial cable are not coupled to the antenna identically, they provide an unbalance. As a result of this unbalanced connection, the amount of current flow I3, displayed in Figure 1, on the outside surface of the outer conductor is dictated by the impedance Zg from the outer shield of the coaxial cable to ground. If Zg is increased to a large enough value, current I3 will be greatly reduced if not eliminated thus providing a clean transition from the coaxial cable to the antenna [2].

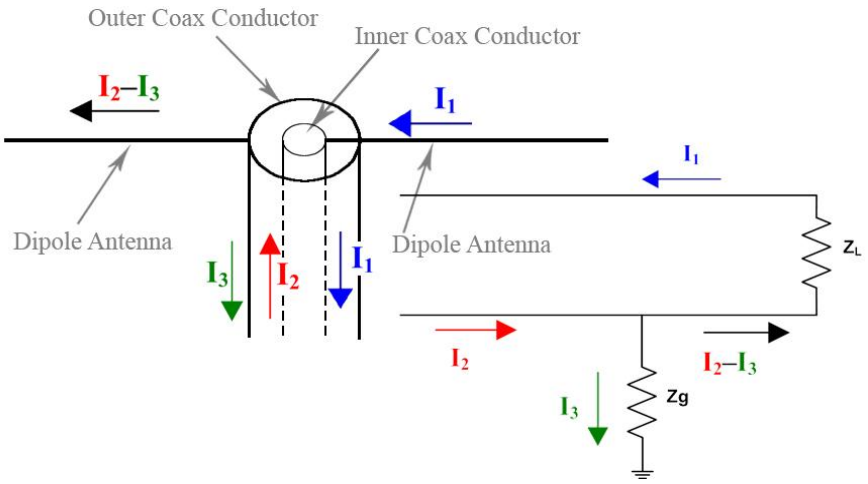

Figure 1: Unbalanced coaxial line with equivalent circuit (edited figure from [2])

A well-known method to avoid this balance problem is to use a coaxial tapered balun by cutting open the outer conductor and tapering it down to a twin wire type structure at the antenna feed. Balun impedance is tapered so that the input reflection coefficient follows a Tchebycheff response in the pass band [3]. This forces the currents on the coaxial cable to be balanced at the end of the wire. As a result, on one end of the balun there is a normal coaxial cable and on the opposite end that feeds the dipole antenna there is a simple two-conductor line seen in Figure 2. The problem with using this design for the TCDA is the length requirement for the taper and manufacturability.

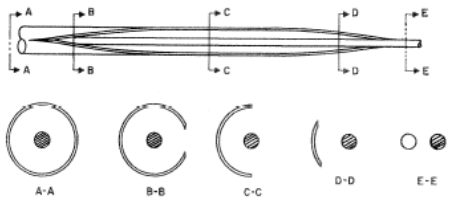

Figure 2: Tapered coaxial balun transformer [3]

1.3. Organization of Thesis

The remainder of this thesis is organized into four parts. Chapter 2 will discuss the common mode problem associated with feeding a tightly coupled dipole array. The common mode problem will be examined and a solution, an enclosed feeding system, will be presented. Chapter 3 presents two wavelength restrictive 180 degree hybrid designs, the Raytheon tapered hybrid and a simple delay line hybrid. An idea to remedy the wavelength restrictions of the delay line hybrid is examined in the analysis of the gap phase reversal hybrid. Chapter 4 presents analysis on an enclosed stripline to twin wire transition. Research is also presented on a dual enclosed stripline structure that is mated to the enclosed stripline to twin wire transition in an effort to create a fully enclosed structure with no wavelength limitations.

CHAPTER 2: TCDA COMMON MODE PROBLEM

2.1. Tightly Coupled Dipole Array

Conventional antenna phased array design usually begins by identifying an antenna with desirable bandwidth and size and placing the element in an array. Usually a spacing of $\frac{\lambda}{4}$ between elements or less is utilized in order to achieve broadside directivity with 0° phase difference between elements and to avoid grating lobes when scanning [2]. However, when the array elements are brought too close to one another, mutual coupling dominates and often results in diminished antenna performance due to impedance

mismatch at the element feed. For the tightly coupled dipole array, the dipole antennas are brought very close to one another creating a tip to tip capacitance. Dr. Benedikt Munk discovered that when this array is brought close to a ground plane at about 0.4λ at the high frequency, the ground plane inductive reactance cancels the array capacitive reactance for low frequencies. At high frequencies, the ground plane capacitive reactance cancels the array's inductive reactance [5] as a result, the antenna is mostly resistive and easily achieves a 4:1 bandwidth. Figure 3 illustrates a unit cell model of a single dipole element over a ground plane as well as a 4x4 element array for L-Band (1GHz – 2GHz).

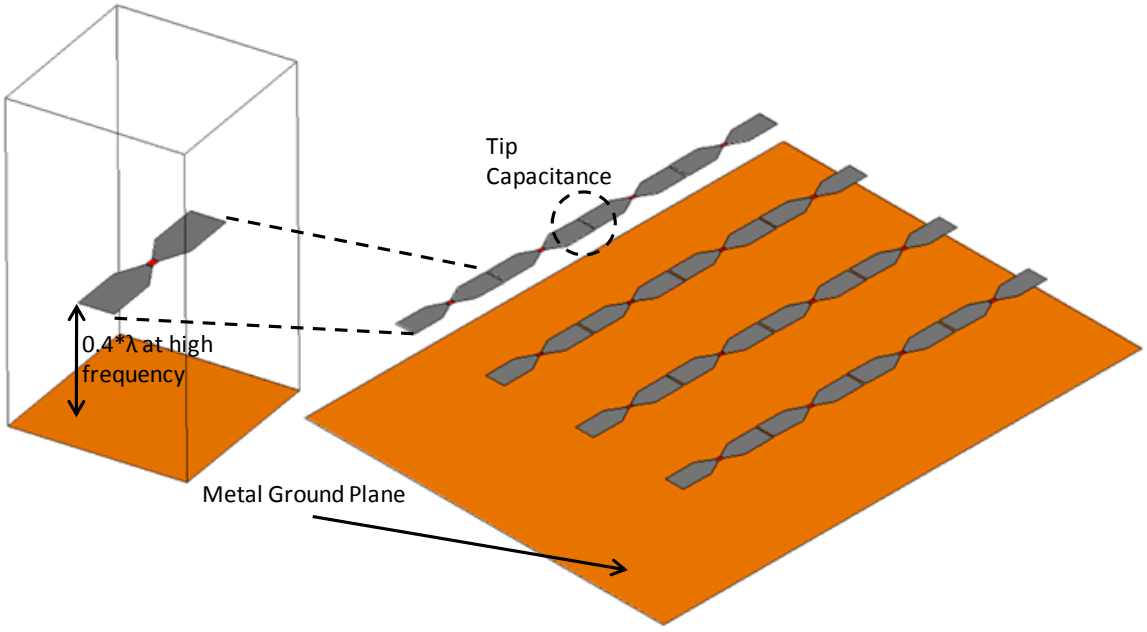

Figure 3: Unit cell model and 4x4 array of TCDA

The elements in Figure 3 are each individually excited utilizing a lumped port. Through parametric analysis by means of unit cell modeling in ANSYS/Ansoft HFSS full

wave simulator, an infinite array is designed. The height above the ground plane is 0.4*λ at 2.5 GHz = 0.4*$\frac{c}{f}$ where c is the speed of light in meters and f is the frequency in hertz which equals 48mm, dipole length = $\frac{\lambda}{2}$ at 2.5 GHz = 60mm, dipole width = 12mm, and the gap between adjacent dipole antennas is 0.127mm (5mil). This design yields a bandwidth of 4.23:1 with an active gamma (Γ) of -10dB or better from 0.6 GHz to 2.54 GHz. Lumped port impedance for each element is 200Ω. It is important to note that unlike a free standing half wave wire dipole antenna which has a radiation resistance of approximately 73Ω, the resistance of a TCDA varies around 200Ω. Active gamma, the Smith Chart, as well as the electric field plot |E| at 2.5 GHz of the unit cell infinite array model are seen in Figures 4 and 5 respectively.

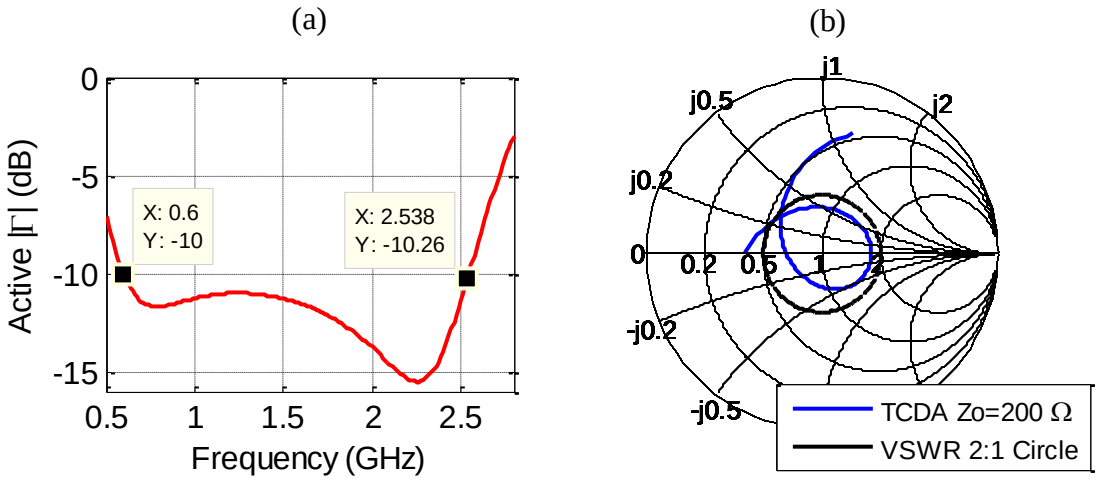

Figure 4: (a) Active |Γ| for TCDA (b) Smith Chart for TCDA normalized to 200Ω

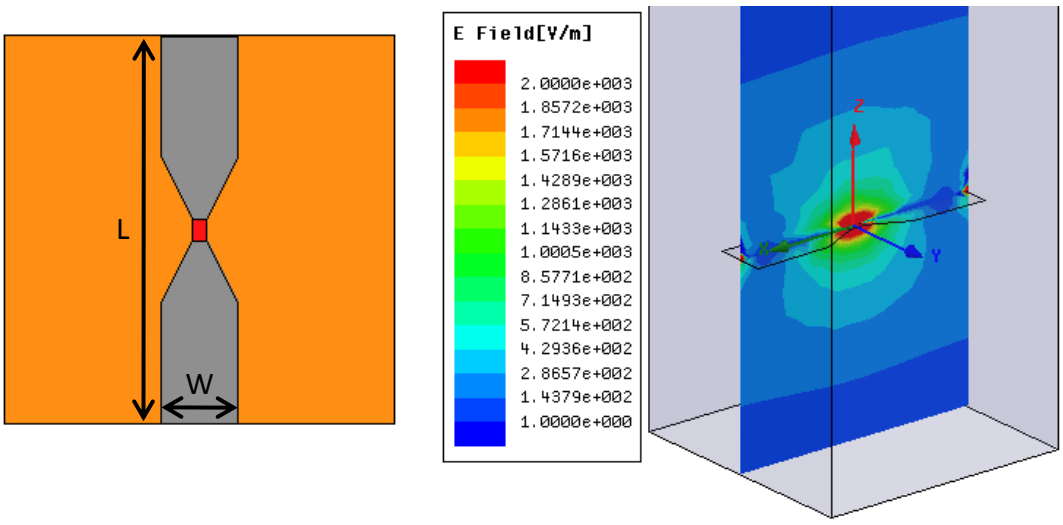

Figure 5: Magnitude of E at 2.5 GHz in the x-z plane

It is interesting to observe that we see a radiation source in three locations on the dipole antenna. One source at the lumped port feed, and on both tips of the dipole where it couples to the neighboring element. This shows that despite the lack of a physical feed at the edge of the dipole, it still acts as another radiating source due to mutual coupling of the active array. Two ideal fictitious methods for feeding the array are discussed in sections 2.2-2.3 below.

2.2. Twin Wire Feed and Common Mode Problem

As discussed in section 1.2, each dipole antenna is a balanced system and operates optimally when excited by a balanced feed. Figure 6(a) demonstrates a unit cell representation of the dipole antenna fed by a twin wire transmission line. The advantage of exciting each array element with a twin wire feed is that the currents on the twin wires are exactly 180° out of phase with respect to one another with equal amplitude which

meets the requirements of a balanced system. The twin wire transmission line is excited by a lumped port just above the ground plane.

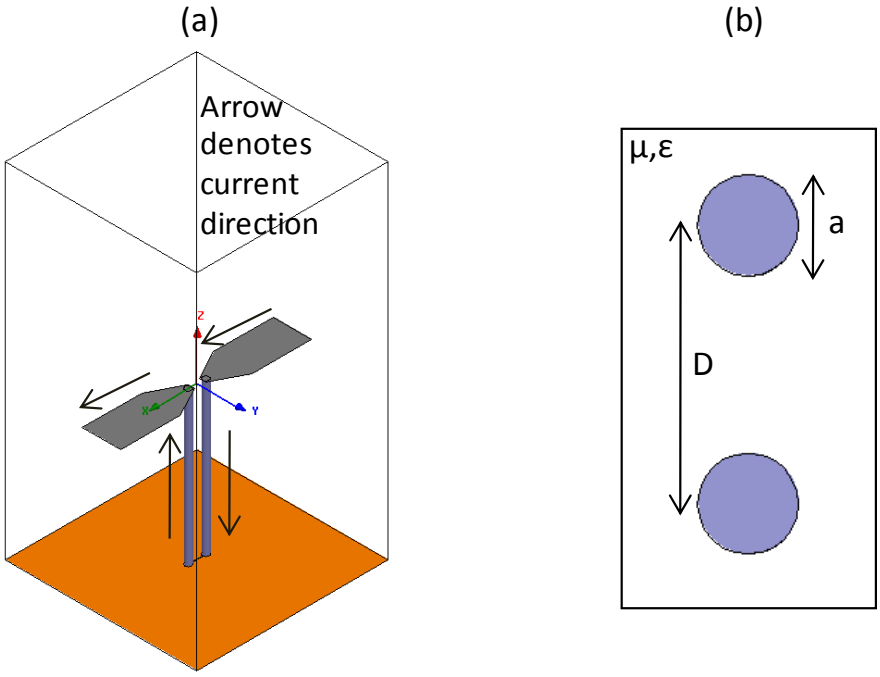

Figure 6: (a) Unit cell of twin wire fed dipole (b) Twin wire top view diameter and spacing

Transmission line resistance was calculated to be 200Ω as follows [6]:

$$L = \left(\frac{\mu}{\pi}\right) * \operatorname{acosh}\left(\frac{D}{2 * a}\right) \qquad C = \frac{\pi * \varepsilon}{\operatorname{acosh}\left(\frac{D}{2 * a}\right)} \qquad R = \sqrt{\frac{L}{C}}\ [\Omega] \qquad \text{[equation 1]}$$

Where μ is the permeability of free space, ε is the permittivity of free space, a is the radius of the conductor in meters, and D is the center to center spacing of the conductors in meters. This is illustrated in Figure 6(b).

This would seem to be an ideal method for feeding the antenna, however there is a fundamental problem with this system. When the length of the dipole arms through the

twin wire feed is equivalent to one wavelength, there no longer exists the differential mode current displayed in Figure 6(a). Rather, there exists a common mode current and the antenna's reflection coefficient reaches 1, causing the gain performance to diminish. This only occurs in the presence of the active array. It is also important to note that this occurs in an ideal situation, where the phase difference on the wires is precisely 180°, there is no amplitude unbalance, yet the common mode problem still exists over a narrow bandwidth. When the phase unbalance at the lumped port feeding the twin wires increases to 5° and 10°, the common mode issue becomes more profound, and slightly wider band. Since it is nearly impossible to fabricate a wide band feed that has no phase or amplitude unbalance over a wide bandwidth, it is important to realize the performance degradation of the twin wire feeding method with 5° and 10° phase unbalance. The common mode problem is illustrated in the surface current vector plot in Figure 7(a) at 1.906GHz on the dipole arms and in Figure 7(b) at 1.85GHz, active $|\Gamma|$ for no phase unbalance, as well as realized co-polarized and cross-polarized gain is seen in Figure 8(a) and 8(b) respectively. This common mode problem also becomes worse when the array is scanned further from broadside. Figure 8(a) shows a spike at 1.906 GHz nearly reaching an active $|\Gamma|$ of 0dB, this problem is reflected in the realized gain plot in Figure 8(b)

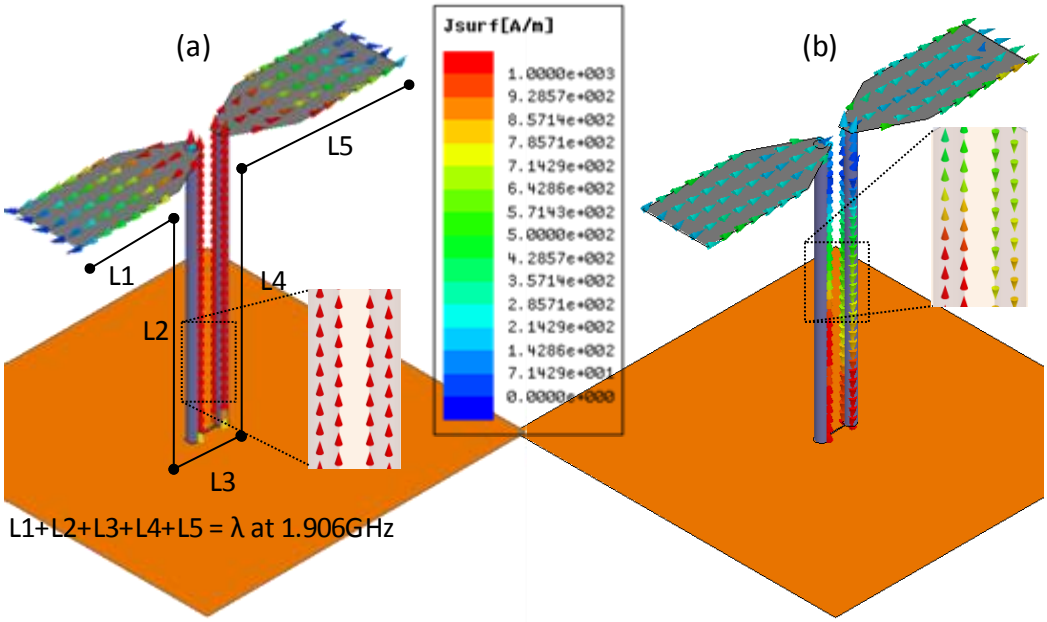

Figure 7: Dipole surface vector current (a) Common mode at 1.906GHz (b) Differential mode at 1.85GHz

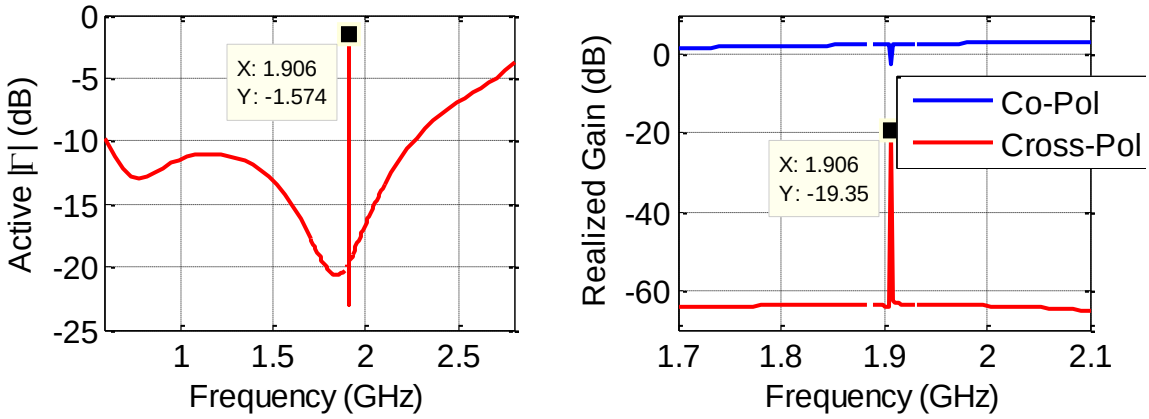

Figure 8: (a) Active |Γ| (b) Realized gain co-polarization and cross-polarization

2.3. Dual Coaxial Balanced Feed

There are multiple different ways to suppress the common mode problem. One can design the array to simply make each element slightly shorter than $\sim\frac{\lambda}{2}$ at the high frequency to push this common mode problem out of the band of operation. However the consequence of this is a greater number of elements per unit area than would have existed otherwise. This has cost implications, not only driving the manufacturing costs of the array up due to extra elements, but more importantly each extra element requires excitation by another transmit/receive module which is expensive. Another method is to use shorting pins close to the feed from each dipole arm to ground to suppress the common mode. The issues with this design is ease of manufacturability, and the introduction of a loop mode that will exist between adjacent array element shorting pins that needs to be controlled/suppressed as well as scan performance limitations.

Ideally a method of feeding that would allow for optimal length for the dipoles, and suppress the common mode without adding any extra complications would be a completely enclosed feeding system. An enclosed structure meaning the entire feed is contained in a metal structure that is unable to radiate and shielded from external forces. The simplest form of this balanced system are two coaxial cables fed 180° out of phase with each outer conductor soldered to one another to cancel any currents that might flow on the outer conductor. This type of feed is displayed in Figure 9 below.

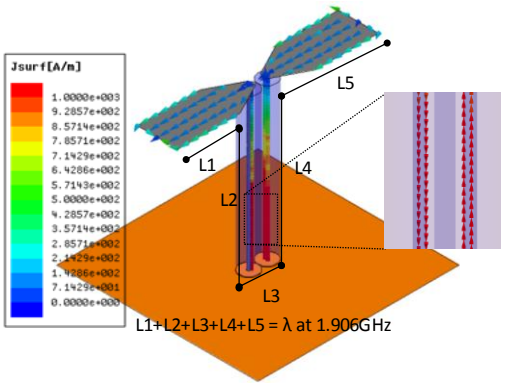

Figure 9: Dual coaxial balanced feed

Each coaxial cable is excited by a wave port right above the ground plane. The outer cylinder is an air "substrate" covered in PEC (Perfect Electric Conductor) on the perimeter but made transparent for ease of illustration. Air was chosen as the material between the conductors in order to keep any existence of a common mode problem at approximately the same frequency as the twin wire case. The impedance of the coaxial cables are 100Ω each, at the feed of the antenna the center conductors add in series giving a 200Ω impedance. Active |Γ| for the unit cell infinite array simulation of the coaxial feed in Figure 9 is shown in Figure 10.

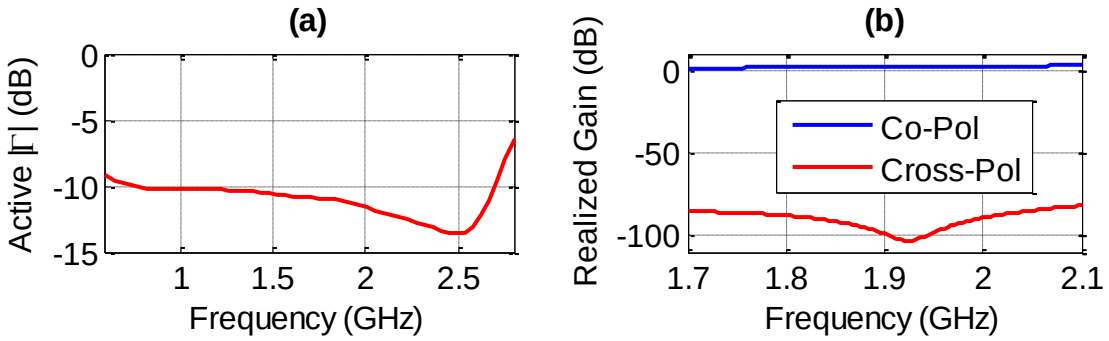

Figure 10: Coaxial feed (a) Active |Γ| (b) Realized gain co-polarization and cross-polarization

Active |Γ| is different from the twin wire case because the array has not been optimized for this feed structure. Figure 10 as well as the vector surface current plot from Figure 9 shows no common mode problem as seen in Figure 8. As a result the remainder of the focus of this paper will concentrate on a feeding structure that will be enclosed, fit in small physical dimensions (unit cell), and be capable of operating in a dual polarization configuration. An ideal stripline based illustration of this full system concept is seen in Figure 11 and Figure 12.

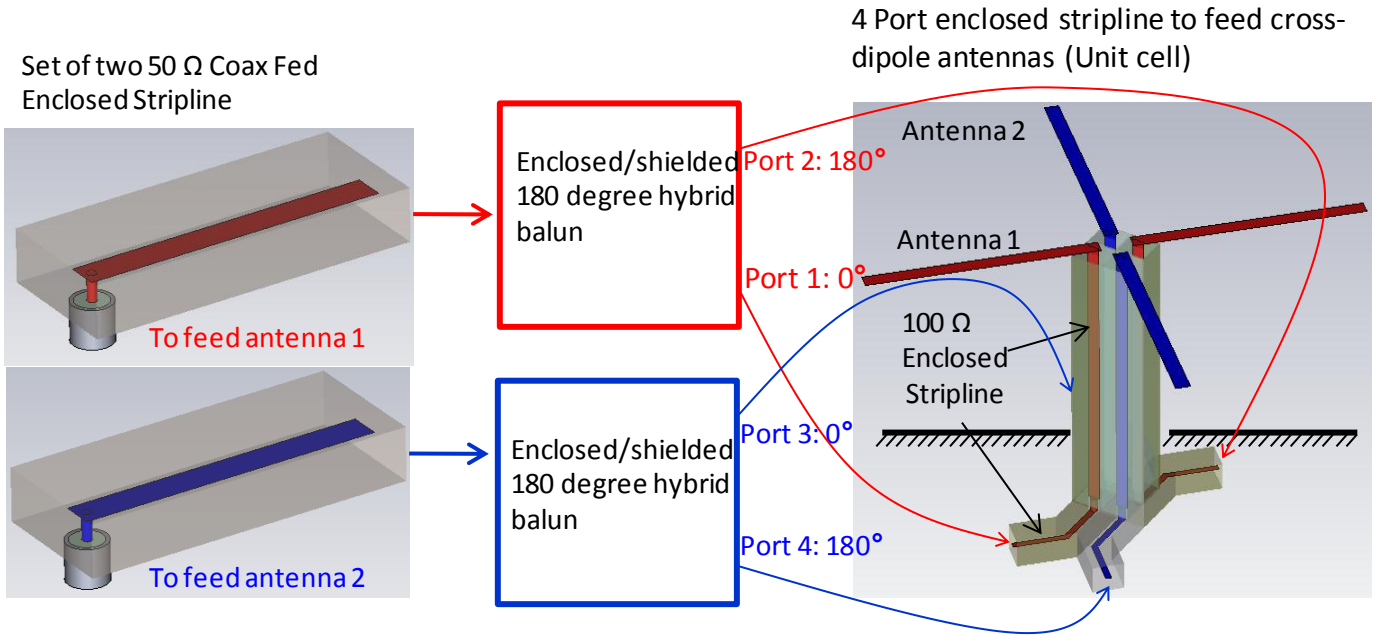

Figure 11: 4 port enclosed unit cell ideal feeding system

Each antenna would be fed by 50Ω coaxial cables directly connected to enclosed stripline, these lines would need to split into two enclosed stripline structures and eventually feed the antenna as shown in Figure 11. Figure 12 shows a front view and top view of the coaxial fed enclosed stripline and 4 port enclosed stripline feed respectively.

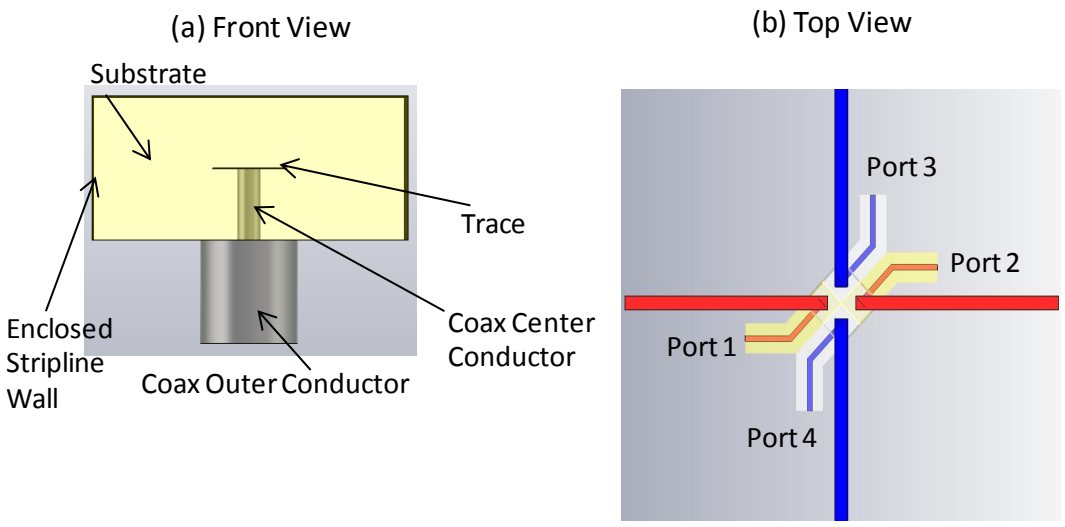

Figure 12: (a) Front view of coax feed from Figure 11 (b) Top view of dipole antenna feed

CHAPTER 3: WAVELENGTH BASED HYBRID AND GAP HYBRID

3.1. Raytheon Tapered Hybrid

Defense contractor Raytheon has an old patent on a three port coaxial fed 180° hybrid based on a tapered microstrip line. This concept was used to create the structure in Figure 13.

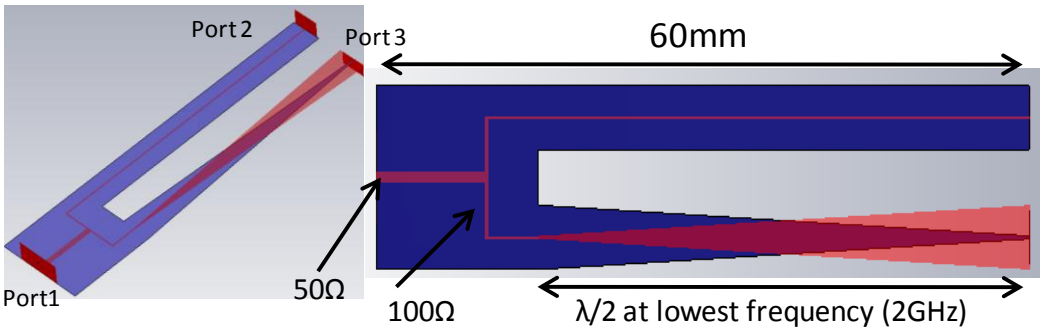

Figure 13: Raytheon based 180° hybrid

The model was built and simulated in CST Studio Suite 2009. This hybrid operates by taking the microstrip trace on one of the 100Ω lines and tapering it out to become the new "ground" plane. Likewise, the ground plane is tapered down to become the microstrip trace. As a result, if a coaxial cable were connected to the ports, it would be connected to port 3 opposite in comparison to port 2. This is easily seen by observing the direction of the wave ports in Figure 13, Port 2 would have the center conductor of the coaxial cable on the top of the board where Port 3 would have the center conductor on the bottom side of the printed circuit board. S-Parameter magnitude and phase is shown in Figure 14 (a) and (b).

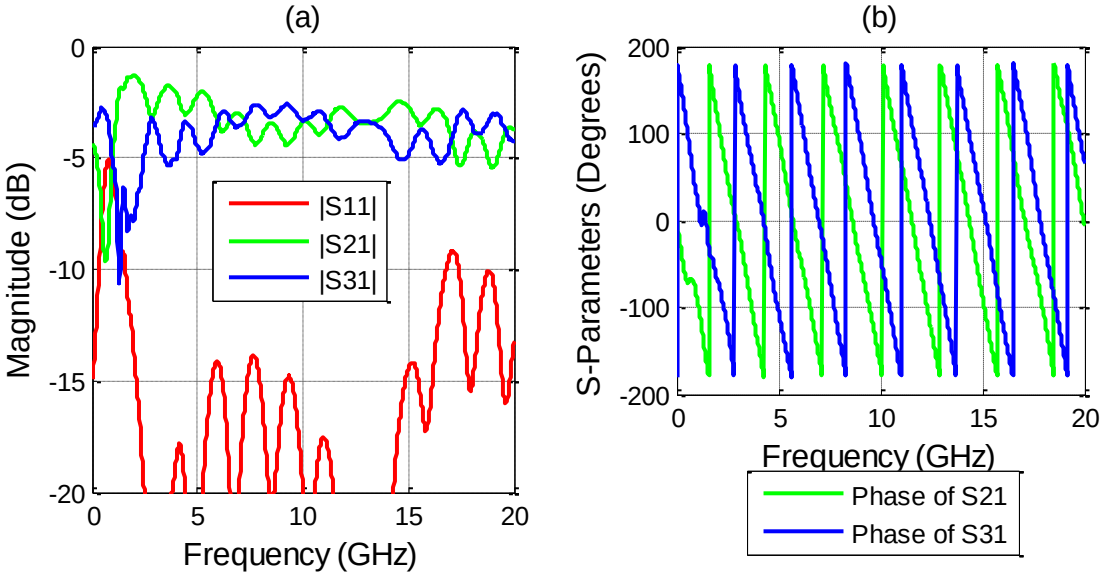

Figure 14: Raytheon Tapered Hybrid S-Parameters (a) Magnitude (b) Phase

It is seen in Figure 14(a) that there is an amplitude unbalance between ports 2 and 3. At some places this unbalanced ripple is as much as 7dB, with |S21| and |S31| often worse than -4dB which is unacceptable. The phase in Figure 14(b) is relatively adequate.

At the low frequencies the phase reversal is ~173°, and at the highest frequencies ~100°. This system could be optimized with a more intelligent taper from 5GHz to 15GHz easily, but the half wave restriction makes it too big. It is difficult to determine how to enclose this structure and mate it with an enclosed stripline transmission line. As a result the Raytheon based tapered hybrid will not be useful for the required application.

3.2. Microstrip Delay Line Hybrid

Typical commercially available hybrids allow for an amplitude unbalance of $\pm$0.5dB to $\pm$0.7dB, as well as a phase unbalance of $\pm$10°. As a baseline for comparison, a simple 180° delay line hybrid was observed. This model was created and analyzed in HFSS. Figure 15 illustrates the model, a simple 50Ω microstrip traces branches off into two 100Ω lines, one of which is 180° ($\lambda/2$) longer than the other.

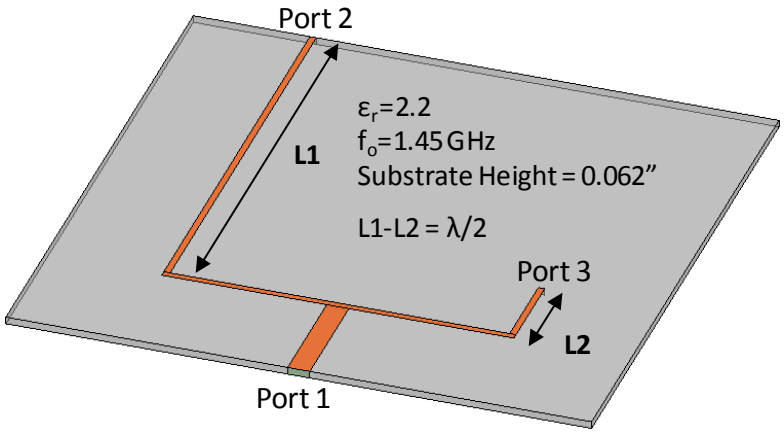

Figure 15: Microstrip Delay Line Hybrid

Since the microstrip line on Port 2 is a half wave longer than the microstrip line on Port 3, there will be a 180° reversal in phase for the wave that reaches Port 2 in

relation to port 3. The phase difference and amplitude unbalance for the delay line hybrid is shown in Figure 16 (a) and (b).

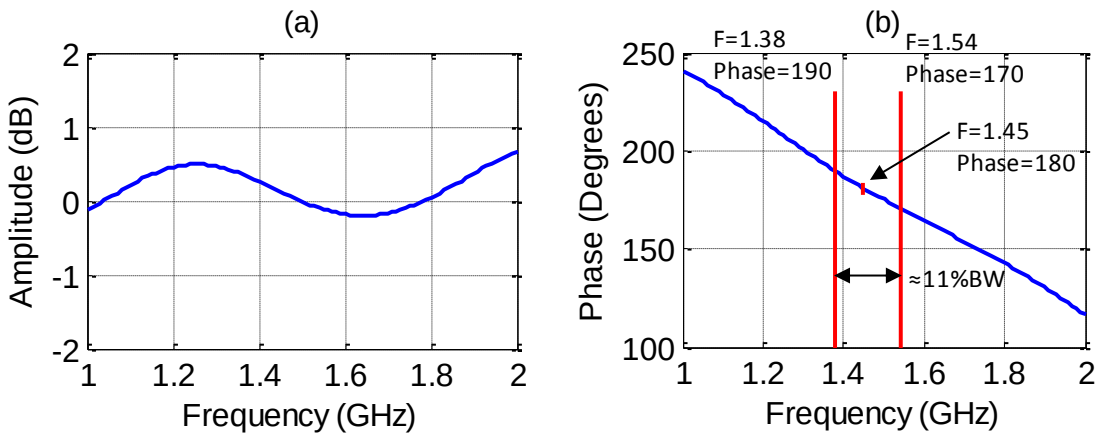

Figure 16: (a) Amplitude unbalance for delay line hybrid |S21|-|S31| (b) Phase difference for delay line hybrid phase(S12)-phase(S31)

It is seen from the amplitude unbalance graph in Figure 16(a) that there is a maximum unbalance at 0.65dB and a minimum at -0.2dB from 1GHz-2GHz which are reasonable values. The $\pm 10°$ phase unbalance in Figure 16(b) is from 1.38GHz-1.54GHz creating an 11% bandwidth of operation for this specification. The delay line hybrid is a narrow band structure that is easily understood and provides a good baseline for comparison of other designs.

3.3. Gap Phase Reversal Hybrid

Thus far, hybrid baluns with wavelength restrictions have been studied. They have been either narrow in bandwidth or require a large amount of space. It would be

more ideal to consider a way to reverse the phase of one of the ports of a 3 port structure without the reliance of a wavelength restrictive. One such structure would be a gap phase reversal hybrid, the concept behind the phase reversal is seen in the cross-sectional view in Figure 17.

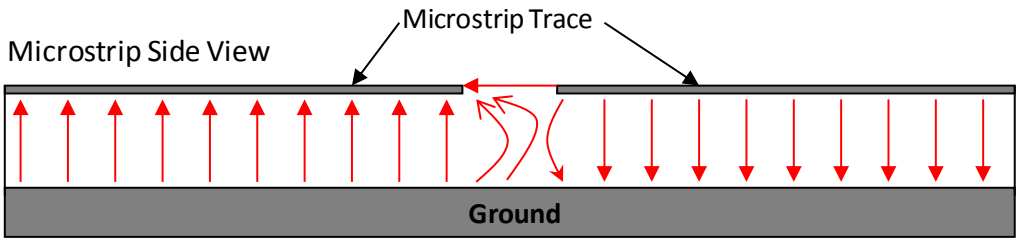

Figure 17: Gap phase reversal concept with E-field vectors

The red arrows represent the electric field lines between the ground plane and microstrip trace. The idea would be to introduce a small gap in the microstrip trace, this would allow fringing fields to occur where the gap exists and force a reversal in phase for the electric fields from one side of the trace to the other. Many commercial 180° hybrids are only useful for specific frequency ranges due to wavelength restrictive designs. If the gap phase reversal occurs as expected, then a perfect 180° phase difference would occur that was not frequency dependent, and thus would be an ultra-wide bandwidth device. The HFSS model and simulation results are seen in Figure 18 and Figure 19 respectively. The hybrid is very similar to that of the delay line hybrid in Figure 15, however all trace lengths are identical, and one trace has a 10mil gap. Simulations were run from 1GHz-2GHz.

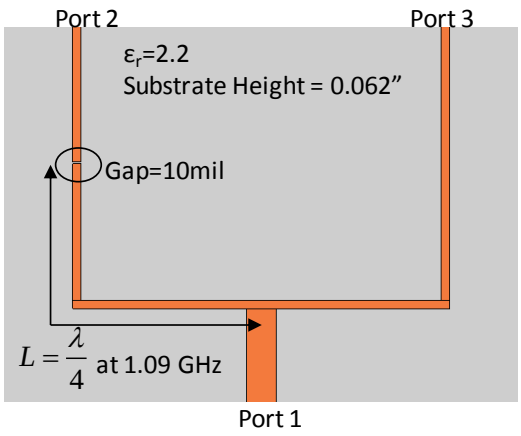

Figure 18: Gap phase reversal hybrid

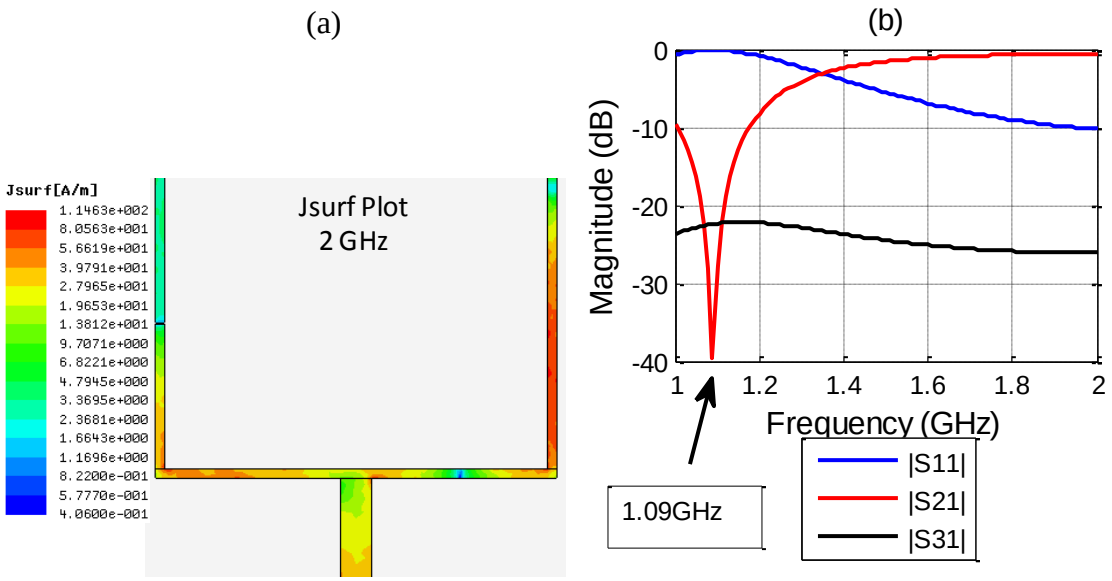

Figure 19: Gap phase reversal hybrid (a) Surface current plot (b) S-Parameter magnitude

Figure 19 shows a problem with this initial design. At 1.09GHz it is seen that |S31| drop significantly. This is due to the fact that the 10mil gap is too large for any power transfer to the other side of the microstrip line. As a result, it appears to the system as an open circuit. Figure 18 shows that the length from the gap to the center of

the trace connected to Port 1 is a quarter wavelength, which transforms this open circuit to a short circuit which accounts for the significant drop at 1.09GHz. The surface current plot in Figure 19(a) shows visually that there is little energy traveling on the trace after the gap. To determine the substrate height and gap width that was necessary for current to transfer across the gap, a parametric study was conducted on a single microstrip trace. The model is displayed in Figure 20 with and without a gap. The gap was varied from 10mil to 0.1mil with a substrate height of 1mm, dielectric constant of 2.2 (lossless), and microstrip trace impedance of 95Ω (1mm width).

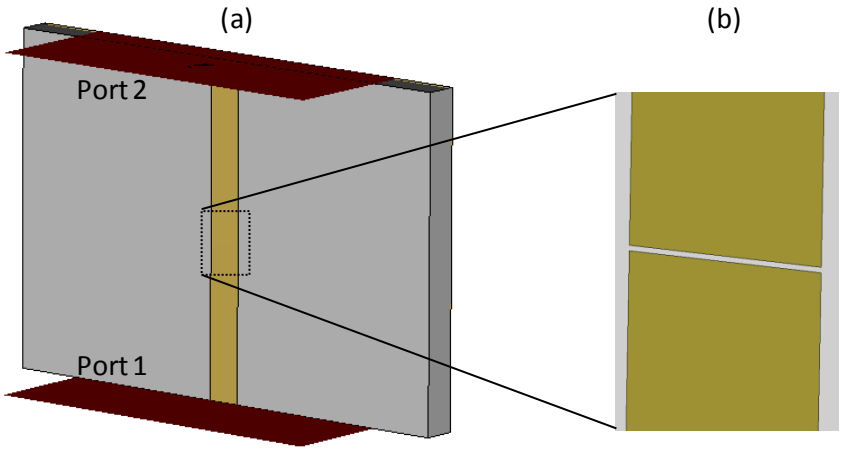

Figure 20: Microstrip with (a) No gap (b) 0.1mil gap

Figure 21 shows the |S-Parameters| for the no gap, 10mil, 5mil, 1mil, and 0.1mil gap cases. Figure 22 compares the phase of S21 for each of these cases. This was simulated in CST Studio Suite 2009, thus a comparison of the time domain pulse is observed in Figure 23 between the no gap and the 0.1 mil gap cases.

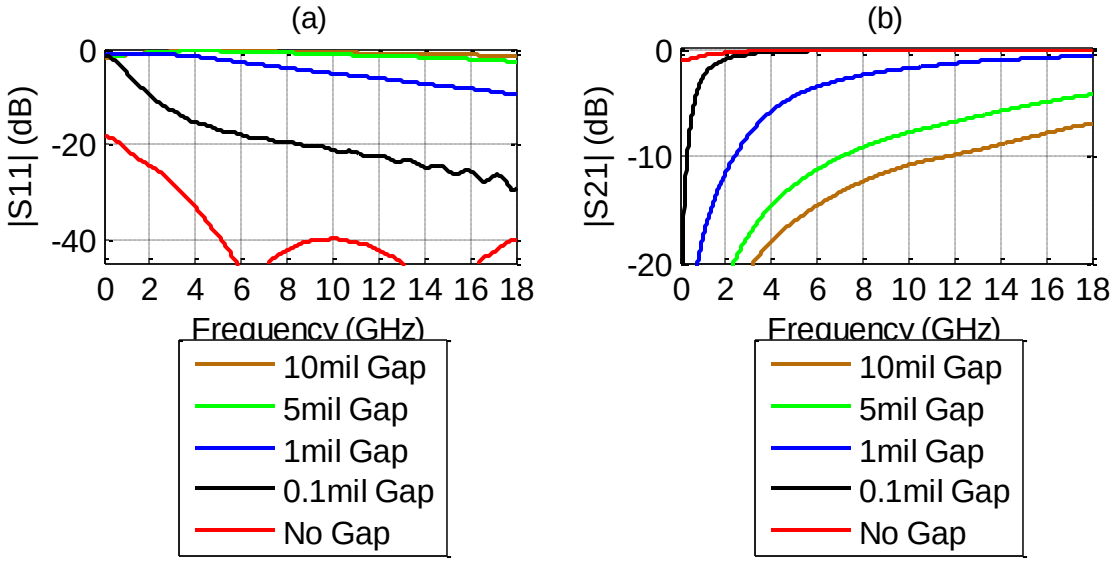

Figure 21: (a) |S11| Comparison (b) |S21| Comparison

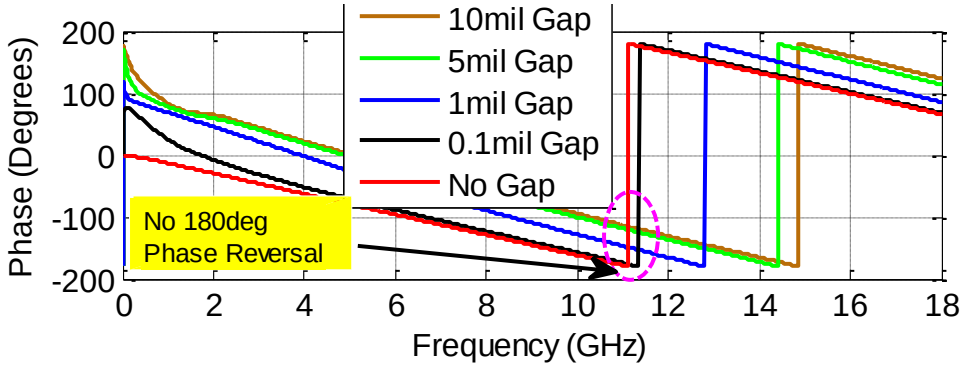

Figure 22: Phase of S21 Comparison

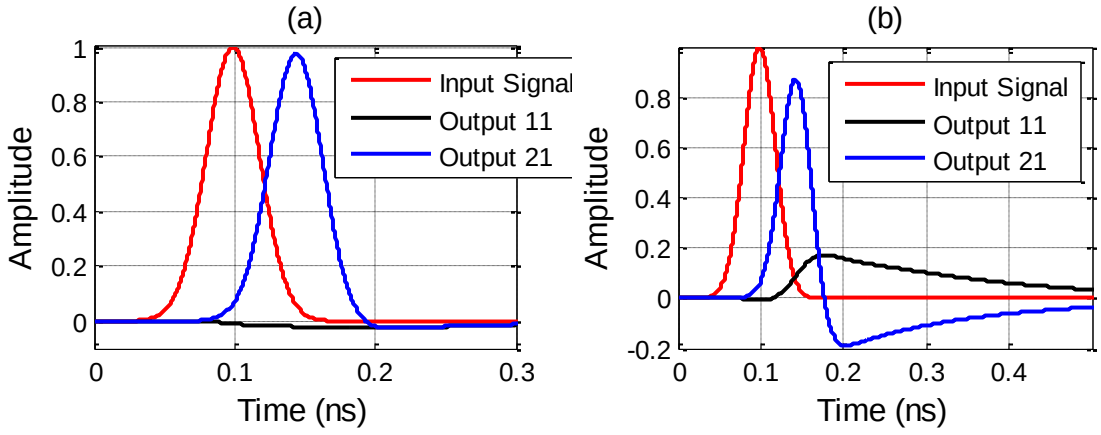

Figure 23: Time domain pulse (a) No gap (b) 0.1mil gap

In Figure 21(a), we see that |S11| is only acceptable (-10dB or better) for the 0.1mil gap case and naturally the no gap case. The same is seen in the |S21| response in Figure 21(b), there is poor power transfer for the 10mil, 5mil, and 1mil cases. Despite significantly better power transfer for the 0.1mil case past 2GHz, there is no phase reversal which is observed in Figure 22. Looking at the time domain pulse of the no gap and 0.1mil gap cases in Figure 23 confirms what is seen in Figure 23, the peak of the output 21 signal drops to 0.8 denoting a reflection which is seen in the output 11 signal. For a 180° phase reversal, the peak of the output 21 signal would ideally need to reach -1 if the input signal were 1.

In order to have reasonable |S21| transfer, the gap must be incredibly small, ~0.1mil, the human hair is 3.3mil in diameter for comparison. The gap is small enough that the fields simply jump over it and do not "see" the gap. It is important to note that typically the smallest size gap that could realistically be milled out of a microstrip trace is on the order of 3mil-5mil, making a 0.1mil gap nearly impossible to fabricate. Despite the small size for the gap, there still is no phase reversal, thus it is concluded that the 180° gap hybrid will not work for this application.

Chapter 4 will begin study of a different frequency non-dependent method for creating the 180° hybrid balun. Ultimately a structure that starts as enclosed stripline will transition into a twinwire transmission line and branch off into two dual enclosed striplines that would feed the antenna. Analysis of this structure will be separated into two portions; the enclosed stripline to twin wire, then the twin wire to dual enclosed stripline. Additionally, this paper will discuss the mating of the two together.

CHAPTER 4: ENCLOSED STRIPLINE TO DUAL ENCLOSED STRIPLINE 180° HYBRID

4.1. Enclosed Stripline to Twin Wire Analysis

Traditional stripline transmission lines consist of a metal trace sandwiched in a substrate between parallel plates above and below the trace. The parallel plates extend for a significant distance when compared to the width of the trace perpendicular to the direction the trace is fabricated in and have the same length running parallel to the trace. The big advantage of the stripline for the required application is that it is a TEM (transverse electromagnetic) transmission line, much like a coaxial cable. As a result it is "non-dispersive", enclosed, and should have no cutoff frequency. The disadvantage is that they are slightly more difficult to fabricate and costly since they require the use of two PCB boards. Another item to note, because the trace is entirely enclosed in a substrate, trace widths are smaller when compared to microstrip since fringing fields are entirely captured in the substrate rather than partially in air and partially in a substrate as in the case of microstrip. This can be an advantage if a small size is required, but a disadvantage if the trace widths become small enough to cause fabrication problems. Traditional stripline impedance can be calculated with the following simplified equation[6]:

$$Zo = \frac{60}{\sqrt{\varepsilon r}} * \ln\left[\frac{4 * H}{0.67 * \pi * W * \left(0.8 + \frac{t}{D}\right)}\right] \qquad \text{[Equation 2]}$$

A cross-sectional view of a stripline transmission line is depicted in Figure 24.

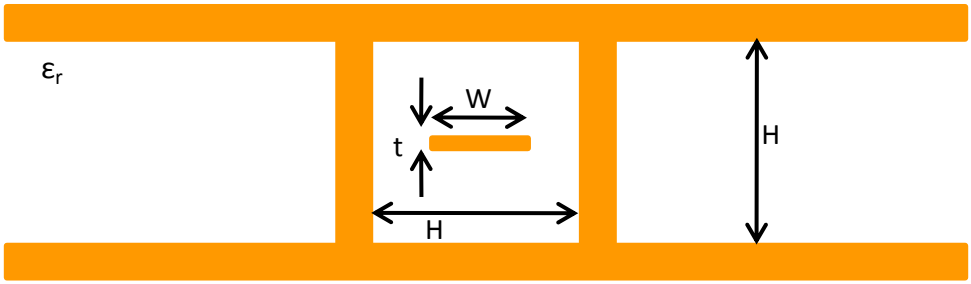

Figure 24: Cross-Sectional view of stripline

The enclosed stripline used for the purpose of this paper would include the vertical lines in Figure 24 thus creating a square wave guide with a trace embedded in the middle. Traditional stripline governed by Equation 2 would not include these vertical lines. It was found that the impedance of the stripline in Figure 24 with the vertical lines was roughly 84.4% of Equation 2.

Two versions of the stripline to twin wire transition are seen in Figure 25. Dimensions listed in the figure are congruent with those displayed in Figure 6(b) and Figure 24. The first is a 50Ω system, and the second is 100Ω. The stripline is excited with a waveport in CST Studio Suite 2009 (this software is used for the remainder of this paper), and a waveport is placed on the end of the twin wire transmission lines. These ports and the PEC walls of the enclosed stripline are made invisible to better illustrate the structure. The stripline impedance was calculated using 84.4% of Equation 2, and the twin wire impedance was calculated using Equation 1. One of the twin wire lines goes through a circular cut in the top of the PEC sheet of the stripline waveguide, and connects to the stripline trace. The other twin wire line connects to the top stripline wall. The idea is to force the current of the trace onto one twin wire, then the current from the stripline

box onto the other twin wire. This would create a differential mode on the wires and result in a balanced twin wire at port 2. S-Parameter results for each model are displayed in Figure 26(a) and Figure (b).

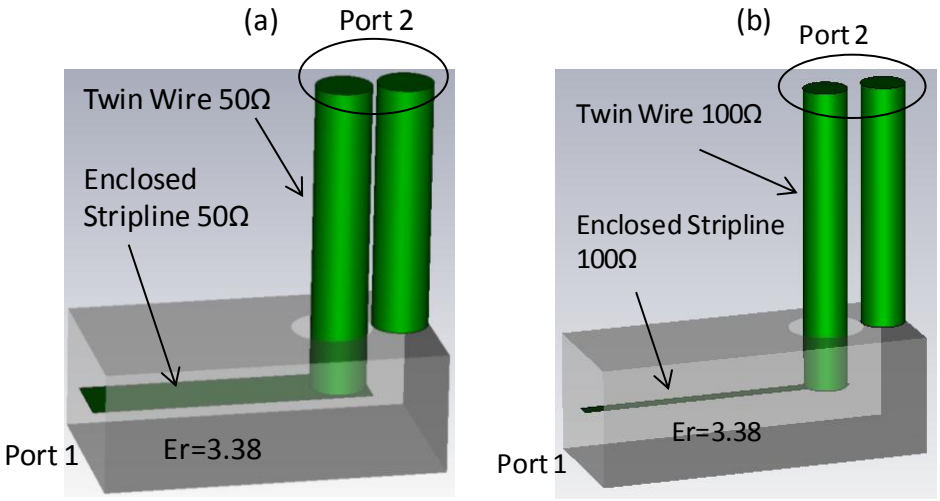

Figure 25: Enclosed stripline to twin wire (a) 50Ω W=0.24mm H=0.6096mm a=0.28mm D=0.305mm (b) 100Ω W=0.07mm H=0.6096mm a=0.225mm D=0.305mm

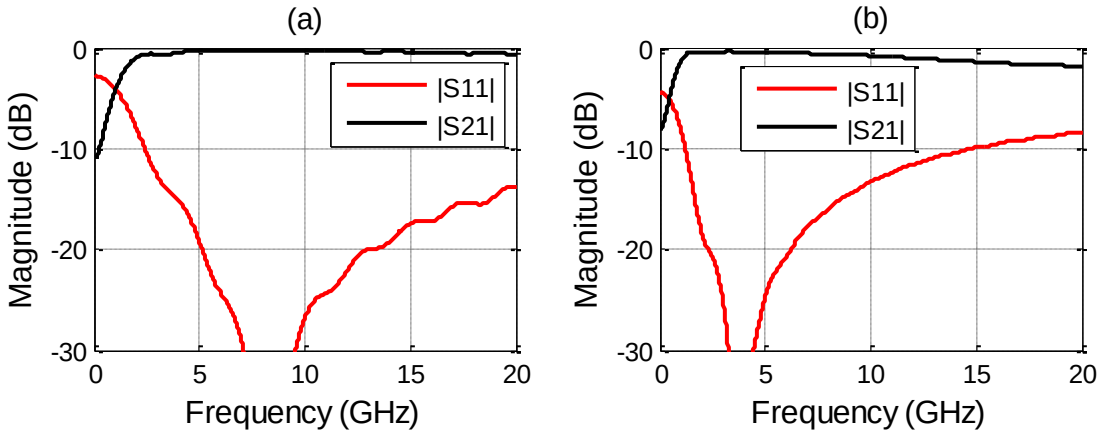

Figure 26: S-Parameters (a) 50Ω system (b) 100Ω system

The 50Ω system performs slightly better than the 100Ω system. |S21| is above -0.5dB from 4GHz to 17.2GHz while maintaining an |S11| of -10dB or less providing a 4.3:1 bandwidth for the 50Ω case. The 100Ω case has |S21| above -0.5dB from 2.7GHz to 5.4GHz while maintaining the same |S11| values for a 2:1 bandwidth. The reason for this difference in performance is demonstrated in the max E-field in time plot in Figure 27.

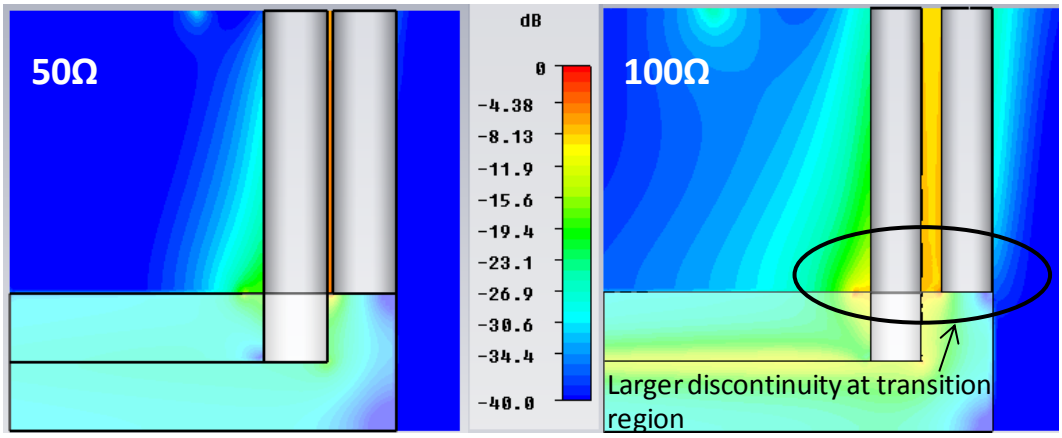

Figure 27: 50Ω and 100Ω max E-field in time

Observing the 50Ω case in Figure 27 we see that the electric fields are indeed tightly coupled between the small gap between the twin wires. There is some radiation at the base of the twin wire that connects to the stripline trace where the hole is cut in the top of the stripline PEC shield. Examination of the 100Ω case tells a different story. To maintain the same D between the wires in the 50Ω case, the 100Ω twin wires must become smaller in diameter to create an impedance of 100Ω since impedance is inversely proportional to the wire radius. This structure needs to eventually connect to dual

enclosed stripline, thus D must be set such that the twin wires sit at approximately the center of the dual enclosed stripline traces. Since the twin wires in the 100Ω case allow for a greater gap between the inner edges of the wires, the electric fields are not as tightly coupled, as a result we see a greater discontinuity at the stripline to twin wire transition when compared to the 50Ω case. The S-Parameter plots in Figure 26 do not give us a feeling for the amplitude or phase unbalance of this system. Section 4.2 will further investigate quantifying this unbalance.

4.2. Quantifying Phase and Amplitude Unbalance of a Twin Wire Transmission Line

In order to quantify the phase and amplitude unbalance of the system in Figure 25, one would need 3 ports, 1 at the input of the stripline, and two at the end of the twin wire transmission line. CST will not allow two wave ports to share the same perpendicular plane and requires at least 1 mesh cell separation between ports. To separate the E-fields between the twin wires and allow for a 3 port system, a small PEC divider is placed between the wires. This is seen in the twin wire system in Figure 28.

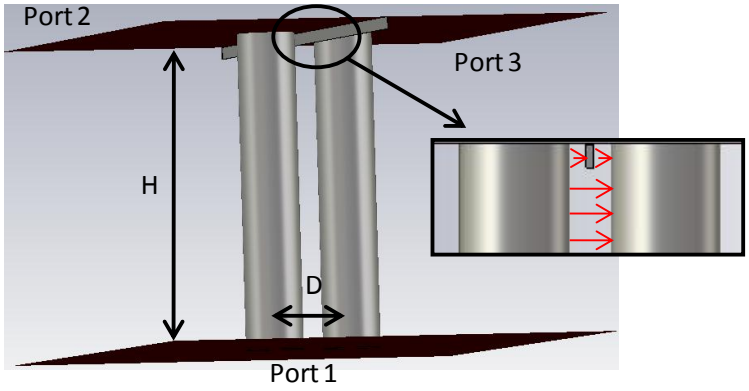

Figure 28: Twin wire with 3 ports and PEC divider a=0.183mm D=0.5mm H=2mm Zo=100Ω

Another requirement of CST is to have the exact same material within a distance of 3 mesh cells in either direction of a wave port, thus the height of the metal plate is made to be 3 mesh cells. The width of the metal plate was varied to X% blockage between the wires and analyzed in Figure 29.

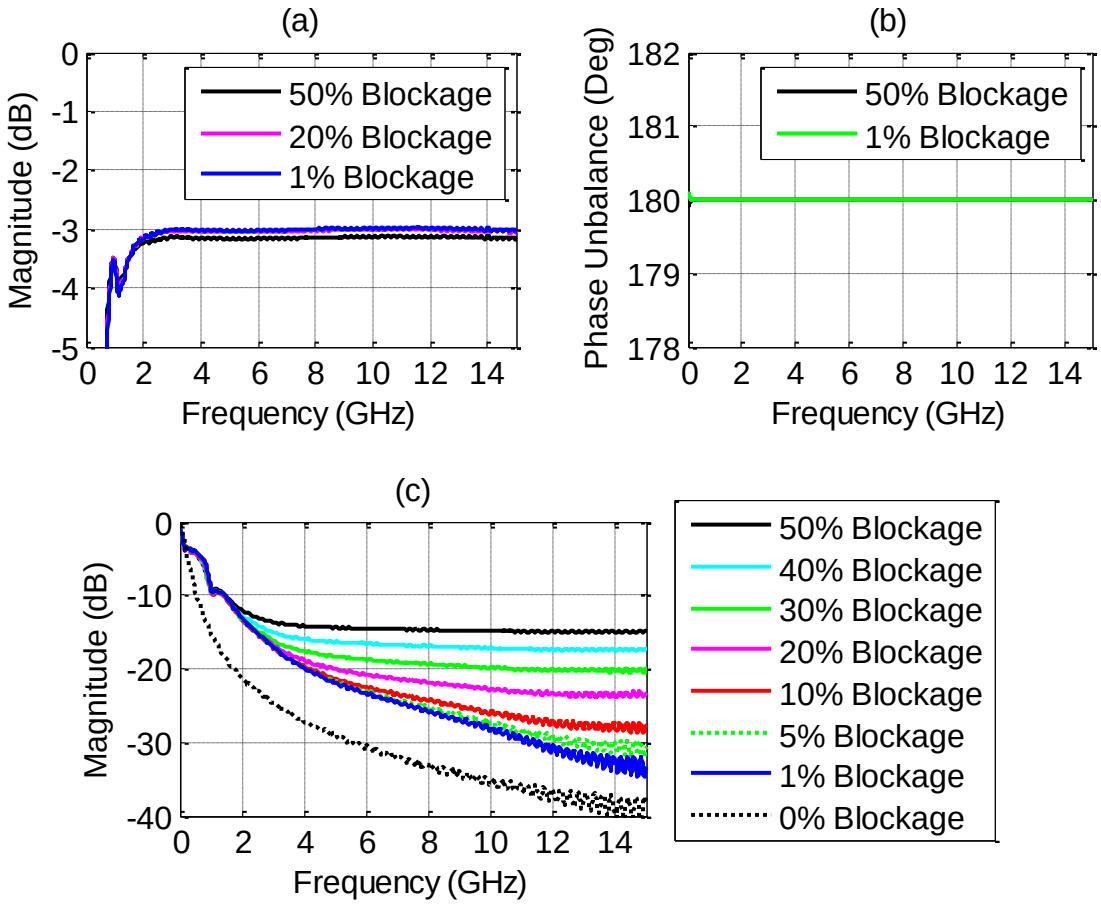

Figure 29: Twin wire 3 port analysis for different percentages of blockage (a) |S21| (b) S21 phase unbalance (c) |S11|

In Figure 29(a) only |S21| is plotted because |S31| is equivalent to |S21|. The twin wire transmission line is inherently ultra-wide band in nature and should not have a low frequency cutoff, the reason for the low frequency cutoff observed in 29(a) and 29(c) is

because the low frequency energy in the system did not die out completely. This is a problem because CST is a FDTD (Finite-Difference Time-Domain) simulation program, and would be remedied by letting the simulation run longer. The metal plate has little significant effect on |S21| or phase unbalance seen in 39(a) and 39(b) even at 50% blockage (phase unbalance for both cases nearly overlap). However, |S11| is affected; the best balance between simulation time and reasonable |S11| was determined to be 20% blockage. The simulation time step on CST is dictated by the smallest feature (i.e. mesh cell), a smaller percentage of blockage relates to a smaller simulation feature which means an increase in simulation time which is why 20% blockage was chosen as it yields an acceptable |S11| of -20dB to simulation time tradeoff. This three port analysis was applied to the models in Figure 25, new models and results are in Figures 30-32.

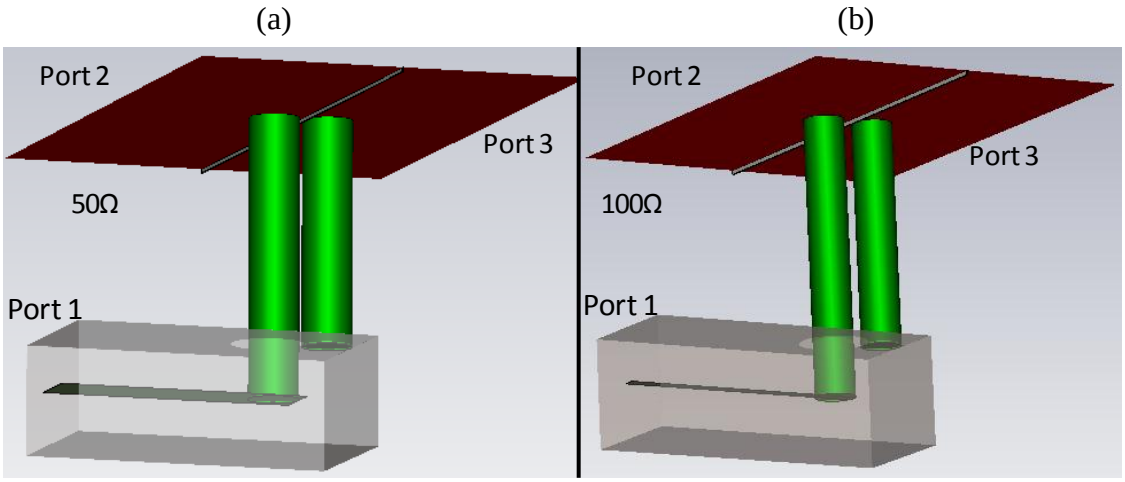

Figure 30: Enclosed stripline to twin wire 3 port analysis (a) 50Ω (b) 100Ω

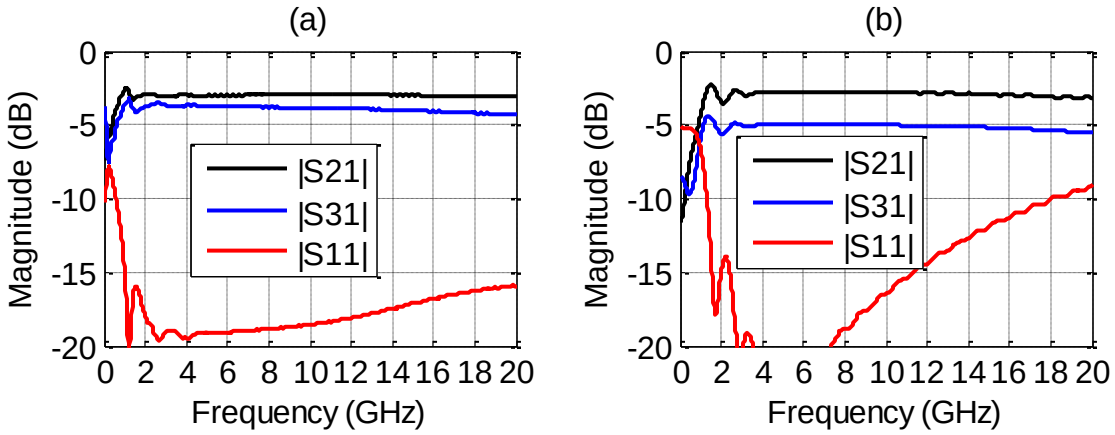

Figure 31: Enclosed stripline to twin wire 3 port |S-Parameters| (a) 100Ω (b) 50Ω

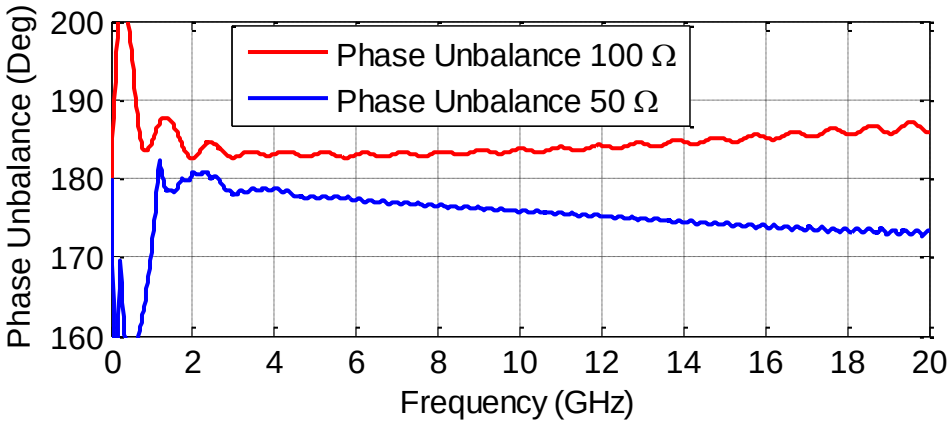

Figure 32: Enclosed stripline to twin wire 3 port phase unbalance (S21-S31)

With the three port analysis of the enclosed stripline to twin wire, we can now quantify the amplitude and phase unbalance. Ideally |S21| = |S31| = -3dB for the S-parameters seen in Figure 31. For the 50Ω case, |S21| is approximately -3dB as expected, however |S31| varies from -3.5dB to -4.2dB over 2GHz to 18GHz, this 0.5dB to 0.7dB unbalance is comparable to the unbalance seen in commercially available hybrids. As seen earlier, the 100Ω transmission lines are worse, |S21| is the expected -3dB for the

majority of the band, |S31| varies from -5dB to -5.4dB from 3GHz to 18GHz. |S11| is -10dB or better over these frequencies for both cases, thus this lower value for |S31| is not due to a miss-match, and it is not due to any conductor/material losses as the model is loss-less. The lower |S31| is due to radiation from the wires at the transition region seen in Figure 27. It is easy to see that there is far more radiation for the 100Ω case as compared to the 50Ω case which accounts for the lowered |S31| values. Phase values in Figure 32 for both cases are acceptable.

Part of the problem with this design is that the current from the enclosed stripline is not equally distributed to the twin wire transmission lines. The stripline trace is directly connected to the left most twin wire in Figure 30, essentially all the current from that trace is transferred to the twin wire. However the right most twin wire does not connect to the entire PEC stripline box, thus it does not receive all the current from the outer shield of the stripline structure. Further, the hole that is cut for the left most twin wire creates a disruption in the currents flowing on the stripline PEC box, some is reflected back to the feed, and some travels around the hole onto the right most twin wire. In short, with this present design, all the current flowing on the stripline PEC box are not forced onto the right most twin wire, there is radiation from the stripline to twin wire transition region causing an amplitude imbalance.

4.3. Twin Wire to Dual Enclosed Stripline Analysis

As mentioned earlier, the configuration in section 4.1 and 4.2 will connect to a dual enclosed stripline structure. The dual enclosed stripline would ultimately become the feeding transmission lines for a single antenna as described in Figure 11. Due to fabrication limitations, an enclosed stripline transmission line could not be built like that shown in Figure 25. Commercially available printed circuit boards contain a substrate with a dielectric constant, with a sheet of copper rolled or deposited onto both sides of the board, and then the metal is milled or etched to create the microwave circuitry. As a result, it would not be feasible to have the metal walls perpendicular to the trace in Figure 25. To relieve this problem, one could create a wall of vias through the multi-layered board that make up the stripline transmission line. Such an enclosed stripline is depicted in Figure 33. Generally the smallest fabricatable diameter size for a via is 5mil with a placement error of no less than 3mil.

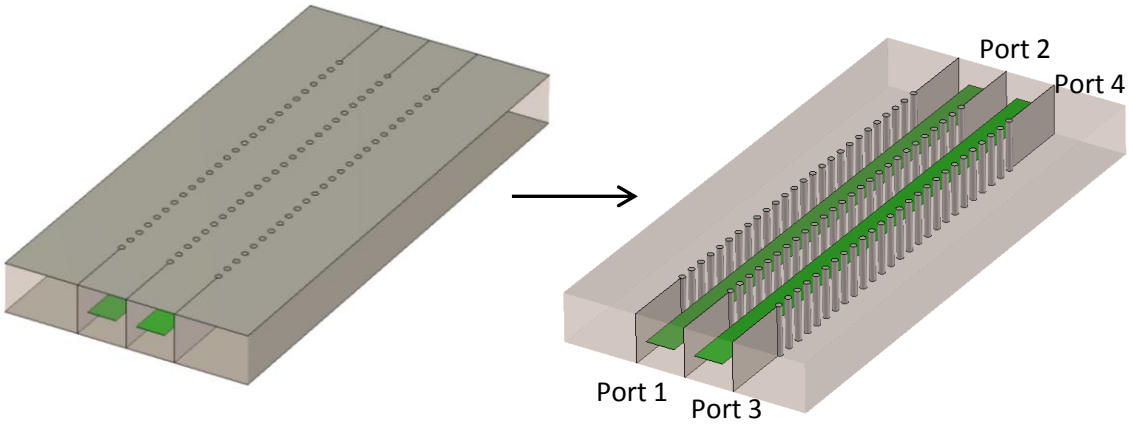

Figure 33: Dual enclosed via stripline - with and without ground planes

Figure 33 shows the dual enclosed stripline, all simulation models displayed through the rest of this paper will have invisible ground planes for illustrative purposes, simulations were run with ground planes. Vertical plates that continue from the vias are left in the model in order to create a proper wave port. Figures 34-35 display the models and results for enclosed via stripline with 3 vias and 26 vias, 0.47*λ and 0.02* λ at 20GHz respectively.

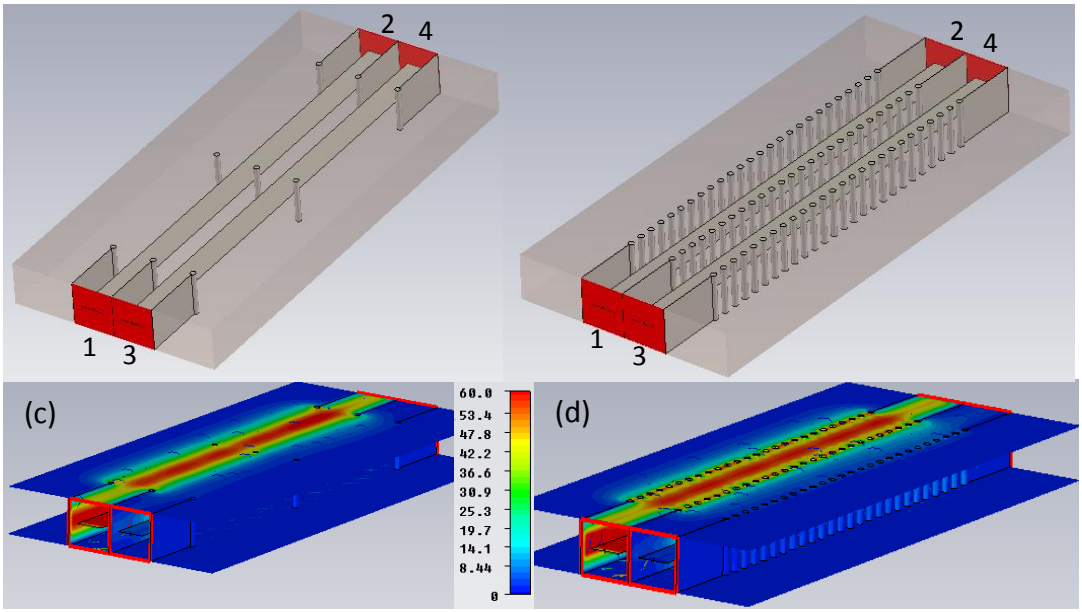

Figure 34: Dual enclosed via stripline (a) 0.47*λ via spacing model (b) 0.02* λ via spacing (c) 0.47* λ via spacing max surface current (d) 0.02* λ via spacing max surface current

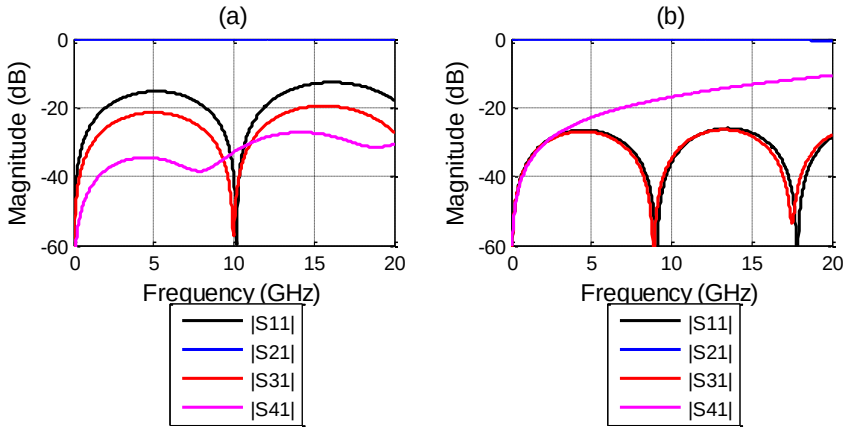

Figure 35: Dual enclosed via stripline |S-Parameters| (a) 0.47*λ (b) 0.02*λ

Figure 35 shows that although there is better isolation between port 3 from port 1, and improved |S11|, |S41| becomes worse. The max surface current plots in Figure 34 (c) and (d) visually shows that there is slightly more energy at the end of port 4 in the case of more vias. One of the difficulties with the via walls versus an actual conducting plate is that the conducting plate is continuous and thus can carry energy much more efficiently. To overcome the limitation of the via walls, and to ensure good isolation between ports 1-2 from ports 3-4, a metal strip is added in the same plane as the stripline strip to short the vias together and make them more continuous. The adjusted model is seen in Figure 36, with simulated data in Figure 37, Figure 35(b) has been copied into Figure 37 for ease of comparison.

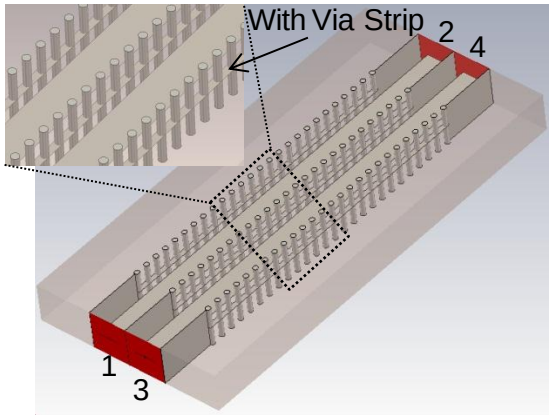

Figure 36: 0.47*λ via spacing with via shorting strip

In Figure 37 we see that all of the S-Parameters improve by adding the shorting strip. Figure 37(c) shows a good improvement in |S21| as well, |S21| of the model in Figure 34(a) varied from -0.4dB to 0dB for comparison.

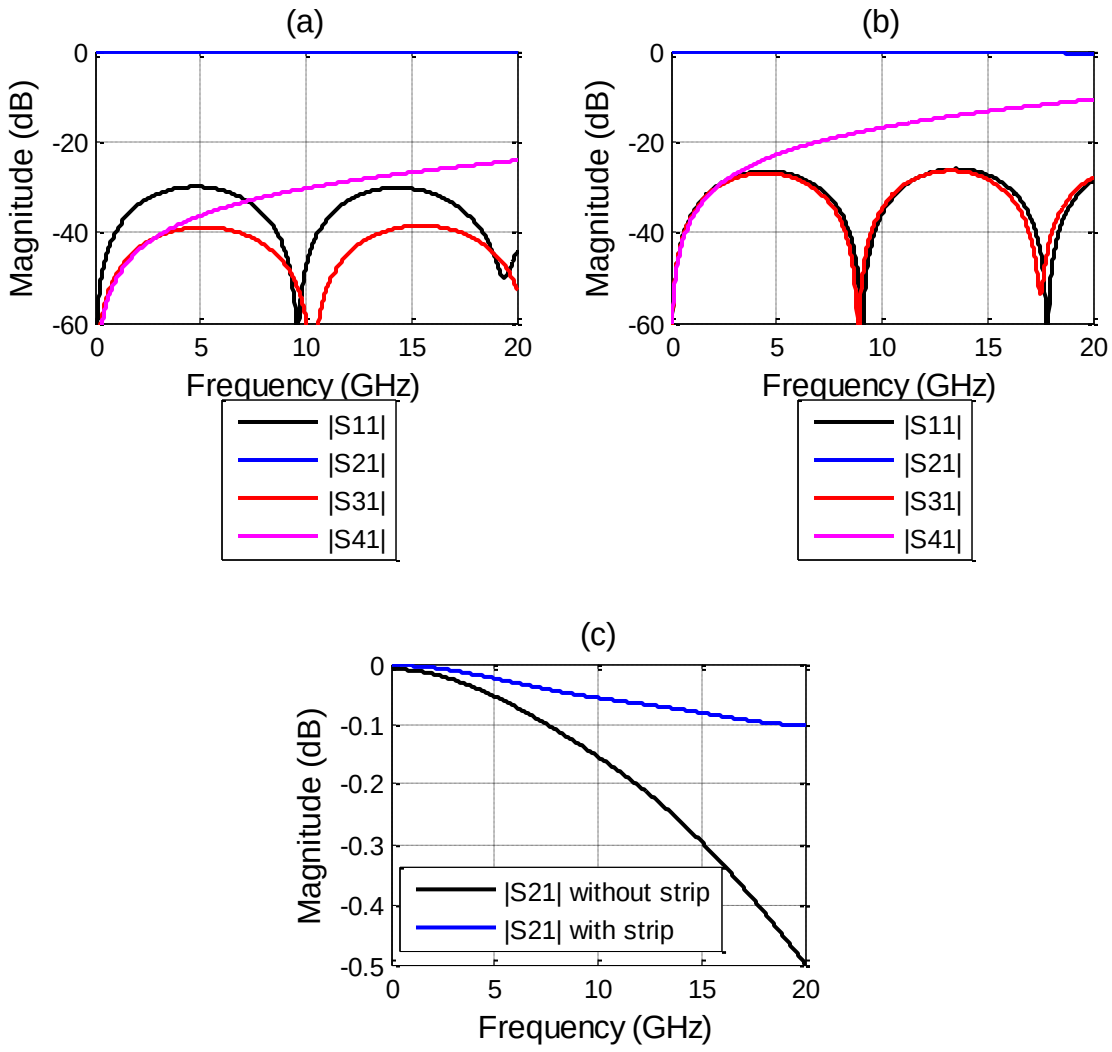

Figure 37: Via enclosed stripline 0.02*λ (a) With shorting strip (b) without shorting strip (c) |S21| compared

Now that the dual enclosed via stripline have been optimized, a twin wire transmission line will be introduced. Ideally the twin wires should have spacing D such that they line up with the center to center spacing of the conducting stripline traces. However, we need the twin wire inner surface distance to be as small as possible as

learned in the 50Ω and 100Ω cases from section 4.1. Models of the twin wire to enclosed via stripline are shown in Figure 38 with results in Figure 39.

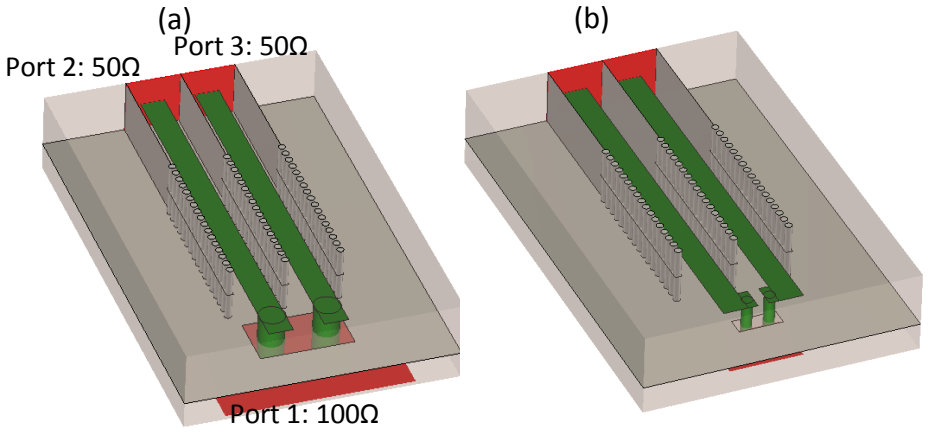

Figure 38: Twin wire to dual enclosed via stripline 100Ω (a) Twin wire D=0.416mm (b) Twin wire D=0.213mm

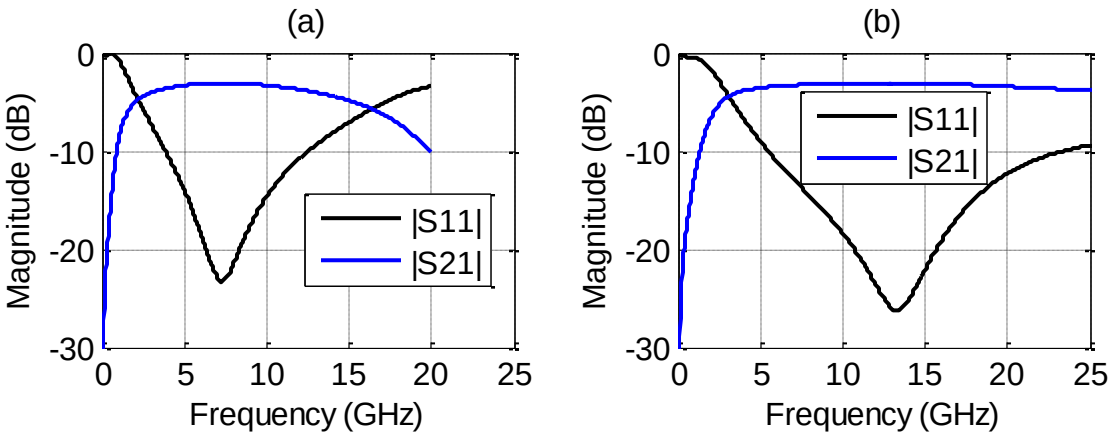

Figure 39: Twin wire to dual enclosed via stripline 100Ω |S-parameters| (a) Twin wire D=0.416mm (b) Twin wire D=0.213mm

Figure 38(a) and results in Figure 39(a) shows the 100Ω twin wire centered on the stripline. |S31| is not displayed in Figure 39 since it is identical to |S21|. |S21| is greater than or equal to -3.5dB from 4.3GHz to 11GHz. Figure 38(b) and Figure 39(b) shows

another 100Ω configuration where the twin wires are brought closer to one another in order to make it possible to connect them to the structure in Figure 25. |S21| is greater than or equal to -3.5dB from 5.2GHz to 21GHz. The configuration in 38(b) is wider in bandwidth and operates at a higher frequency because the wires are closer to one another. Since the wires are closer, and the rectangular cut in the box is larger in proportion to their spacing, there is better transfer of the electric fields from one wire to the other. Thus it becomes necessary to ensure the hole cut in the ground plane is optimized in width and length to enable optimal twin wire performance.

Only a 100Ω configuration is shown for a couple of different reasons. Although we learned that the 50Ω system performs better for the enclosed stripline to twin wire transition from Figure 25, the TCDA naturally operates around 200Ω and would be easier to re-design to operate at 100Ω rather than 50Ω. Also, the 50Ω twin wire would be split into two 25Ω enclosed stripline traces rather than 50Ω. The consequence of this are traces that are much wider and it is no longer possible to have a square shaped enclosed stripline structure, rather there would need to be a rectangular shaped enclosed stripline forcing longer tabs as those seen on Figure 38 (b). The problem with longer tabs is that the junction seen at the terminals of the twin wire transmission lines is seen by the striplines as a parallel circuit, and thus would be 50Ω||50Ω = 25Ω much like the microstrip traces in Figure 15 where 100Ω||100Ω=50Ω, not 100Ω which is the characteristic impedance of the twin wires. The configuration in Figure 38(a) allows the twin wire impedance to be split as a series circuit, not a parallel circuit. As a result having longer tabs creates two sets of transmission lines that see the feed of the twin

wires oppositely. The reason a 200Ω system is not analyzed is due to inner surfaces of the twin wire being farther apart from one another amplifying the twin wire radiation problem seen in the 100Ω case in Figure 27 when transitioning from stripline to twin wire.

4.4. Enclosed Stripline to Dual Enclosed Stripline Mated

The twin wire to dual enclosed via stripline from Figure 38(b) is mated with the enclosed stripline to twin wire from Figure 25(b), model and results are in Figures 40-41.

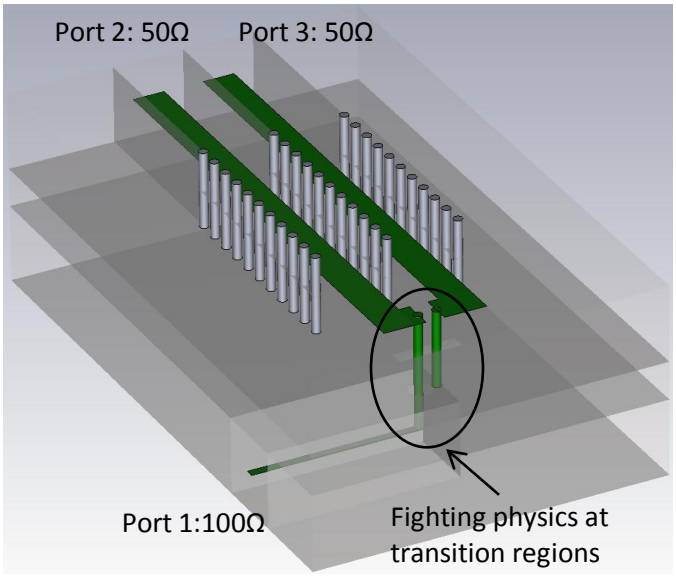

Figure 40: Enclosed stripline to twin wire to dual enclosed via stripline

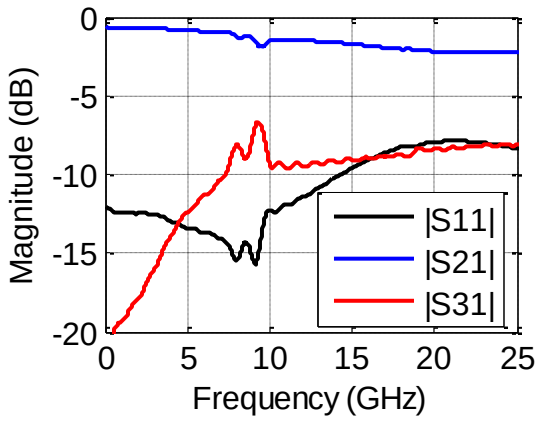

Figure 41: Enclosed stripline to twin wire to dual enclosed via stripline |S-parameters|

Unfortunately the S-parameters in Figure 41 are not adequate. In short, there is a huge amplitude unbalance between Port 2 and Port 3. There is little current flowing onto the right most twin wire accounting for the limited power transfer at Port 3. Also, |S11| is poor due to the transition region circled in Figure 40. The inner surface of the twin wires need to be as close as possible to one another, however, the enclosed stripline from ports 2 and 3 have the problem described above when tabs are added at the twin wire feed, and the traces can only be so close to one another. The inner surface distance (gap) of the twin wires from Figure 40 and Figure 38(b) is 12 mil, 16 mil gap is observed in Figure 38(a), the gap for the 50Ω and 100Ω cases from Figure 25 are 1mil and 3mil respectively. This means that the unbalance/radiation problem observed in Figure 27 will be worse in Figure 40 due to the larger gap. Regrettably, this non-wavelength restrictive system will not provide the performance required to feed the TCDA.

CHAPTER 5: CONCLUSION AND FUTURE WORK

Several different 180° hybrid balun structures are analyzed in this paper. For the unit cell applications of the tightly coupled dipole array, it is ideal to have a non-wavelength restrictive structure. The Raytheon hybrid could provide the required performance however it is to large due to the half wave restriction. The simple delay line hybrid provides a good narrow band and easy to understand basis for analysis and performance to compare other hybrids to. The gap hybrid would be a good wavelength non-restrictive structure, however in order to have sufficient power transfer through the microstrip trace gap, an un-realizable small gap must be fabricated. Further, there is no 180° phase reversal between the output ports of the gap hybrid. The full enclosed stripline to twin wire to dual enclosed via stripline looks promising when analyzed as two separate structures. When mated, the transition regions containing the twin wire fights physics and have poor performance.

Current TCDA technology is bottle necked by feeding structures that either limit bandwidth, limit scan angles, or contain a common mode problem. The only way this technology will advance is through a novel feed design. Thus, there still remains work to be done to develop a wide band enclosed balun transformer for the tightly coupled dipole array. It may be easier to create such a structure that works for the L-Band array presented in section 2.1 rather than an X-Band array since the unit cell is larger providing more room for a non-wavelength restrictive balun. Whether a wavelength or non-wavelength restrictive solution is investigated in the future, it may be necessary to ensure it is an enclosed structure to help avoid the common mode problem of the TCDA not only

at broadside but also when scanning the phased array. If an enclosed structure is not possible, then some other means of avoiding the common mode problem should be developed that does not increase the cost of the array.

REFERENCES

[1] Kasemodel, J.A.; Chi-Chih Chen; Volakis, J.L.; , "Wideband Planar Array with Integrated Feed and Matching Network for Wide-Angle Scanning," *IEEE Transactions on Antennas and Propagation, 2010.* (currently under review)

[2] Balanis, Constantine A. Antenna theory analysis and design. New York: Wiley, Ch. 6 & Ch. 9, 1997.

[3] Duncan, J.W., and V.P. Minerva. "100:1 Bandwidth Balun Transformer." Proceedings of the IRE 48 (1960): 156-64.

[4] Kasemodel, J.A.; Chi-Chih Chen; Volakis, J.L.; , "A miniaturization technique for wideband tightly coupled phased arrays," *Antennas and Propagation Society International Symposium, 2009. APSURSI '09. IEEE* , vol., no., pp.1-4, 1-5 June 2009

[5] Munk, B.; Taylor, R.; Durharn, T.; Croswell, W.; Pigon, B.; Boozer, R.; Brown, S.; Jones, M.; Pryor, J.; Ortiz, S.; Rawnick, J.; Krebs, K.; Vanstrum, M.; Gothard, G.; Wiebelt, D.; , "A low-profile broadband phased array antenna," *Antennas and Propagation Society International Symposium, 2003. IEEE* , vol.2, no., pp. 448- 451 vol.2, 22-27 June 2003

[6] Pozar, David M. “Chapter 2: Transmission Line Theory.”, "Chapter 3: Transmission Lines and Waveguides." *Microwave Engineering*. Hoboken, NJ: J. Wiley, 2005. 55,137-142.